PHYSICAL REVIEW A VOLUME 27, NUMBER 6 JUNE 1983

The neutron scattering function for hard spheres

W. E. Alley and B. J. Alder
Lawrence Livermore National Laboratory, University of California, Livermore, California 94550

Sidney Yip
Department of Nuclear Engineering, Massachusetts Institute of Technology, Cambridge, Massachusetts 02139
(Received 6 December 1982)

Density, longitudinal, and transverse-current correlation functions for hard spheres at various densities and wavelengths have been generated by computer simulation and compared with both the generalized Enskog kinetic theory and wavelength-dependent hydrodynamics. It is shown that even for dense gases the generalized Enskog kinetic theory is quantitatively accurate in describing the thermal fluctuations at finite wavelengths and frequencies, as is wavelength-dependent hydrodynamics, as long as the wavelength is greater than the mean free path. At liquid densities neither theory can account for the viscoelastic relaxation effects, directly observed in the transverse-current correlation function by shear-wave propagation, at a wavelength somewhat above the first diffraction maximum. However, wavelength-dependent hydrodynamics quantitatively describes the neutron scattering function at wavelengths from this point (above the first diffraction maximum) through the diffraction maximum (where the de Gennes narrowing occurs) to the mean-free-path limit. Furthermore, viscoelastic effects in the long-wavelength regime can be accounted for by introducing into hydrodynamics time-dependent transport coefficients. At still longer wavelengths, viscoelastic relaxation times become short compared with hydrodynamic relaxation times and ordinary hydrodynamics with constant transport coefficients describes the neutron scattering function.

I. INTRODUCTION

The dissipation and propagation of spontaneous fluctuations in a classical fluid at thermal equilibrium can be experimentally investigated by neutron and light scattering or simulated by computer molecular dynamics. Simulation has the advantage that it produces results of a specified accuracy for a known simple intermolecular potential and, hence, lends itself well to a quantitative test of nonequilibrium theories and models. These theories[1,2] of the dynamic processes in fluids have been developed either at the macroscopic or continuum hydrodynamic level,[3,4] or at the molecular or kinetic level.[4,5] The purpose of this paper is to establish the domains of validity of these two reference theories and the quantitative differences in the intermediate distance and time regime which more complex theories must take into account.

In either of these two theories a generalized version needs to be employed since we want to predict the time evolution of a wavelength-dependent property rather than just the time evolution of a correlation function in the long-wavelength limit which leads to an ordinary transport coefficient. The generalized or wavelength-dependent kinetic theory is based on Enskog's modification of the Boltzmann equation which takes into account the finite size of the hard spheres relative to the average distance between particles.[6,7] The accurate numerical solution of this generalized kinetic equation is elaborate and has been given in a separate paper.[8] Since it was previously found that the generalized Enskog model predicts quite accurately (for all but very dense fluids) the generalized transport coefficients,[9] it can be anticipated that the neutron scattering function will be quantitatively reproduced at all but liquid densities. Even at liquid densities, at sufficiently short wavelength, the generalized Enskog model becomes exact since under these circumstances correlated collisions can be neglected. Attempts to extend kinetic theory through consideration of such correlated collisions will not be considered here.

Hydrodynamics is generalized only to the extent of including wavelength-dependent thermodynamic and transport coefficients so as to predict the decay of the fluctuations. The term generalized hydrodynamics implies both wavelength- and frequency-

dependent transport coefficients. If we were to introduce the frequency dependence of the transport coefficients as well we would have a tautology since such frequency- and wavelength-dependent transport coefficients were themselves derived from the decay of the various types of fluctuations. Indeed, the objective of utilizing only wavelength-dependent transport coefficients is to clearly delineate the region in wavelength where the time dependence of the transport coefficients can be neglected; namely, the region where the hydrodynamic relaxation times are much longer than the relaxation times associated with the autocorrelation function of the various transport coefficients. This spatially nonlocal hydrodynamics has the further limitation that it is only applicable for fluctuations of small amplitude since the wavelength-dependent properties were derived from a linear theory. Furthermore, the continuum model must be expected to break down unless tha wavelength is at least larger than the mean free path. Since the mean free path at liquid densities is an order of magnitude smaller than the diameter of the particle, it appears optimistic to expect the continuum approximation to hold to such small distances; however, for dynamic properties the mean free path is the relevant length scale.

Previous attempts have been made to introduce wavelength dependence into hydrodynamics but only in a limited sense. The most obvious way is to introduce wavelength-dependent thermodynamic properties but ignore the wavelength dependence of the transport coefficients.[10] This is accomplished through the static structure factor and the thermodynamic properties that can be derived from it, such as the isothermal compressibility and the sound speed. This procedure, however, ignores the wavelength dependence that arises at finite wavelength through the coupling of energy and density fluctuations. This coupling leads to a transport mechanism whose effect vanishes at long wavelengths, but at finite wavelengths affects such thermodynamic properties which in the long-wavelength limit become, for example, the temperature derivative of the density or the heat capacity at constant pressure.

Some of the details of the computer molecular-dynamics calculations are given in Sec. II. Section III gives the comparison to the two theories at a series of densities, wavelengths, and frequencies in graphical form and discusses the discrepancies. This comparison is restricted to hard spheres since only for them are the generalized kinetic theory and generalized transport coefficients presently available. In Sec. IV the question is addressed as to whether it is possible to detect the effect of the long-time tail of the transport coefficients in the neutron scattering function through the dependence of the sound speed on wavelength. In Sec. V the transverse-current correlation function is described. In the Appendix the intermediate-scattering function and the transverse-current correlation function for hard spheres, as calculated by molecular dynamics at two densities and a few wave numbers, are tabulated.

II. MOLECULAR-DYNAMICS SIMULATION

The simulations were carried out on a system of N particles contained in a periodically repeated cubic cell. For most of the runs N was 500, but a few runs at $N=4000$ were also carried out to check the number dependence on a system that is of exactly twice the linear dimension and thus contains exactly commensurate wavelengths. The length of the cube was chosen to be unity and the hard-sphere diameter σ was varied to give the desired density. It is convenient to specify density by the volume ratio V/V_0, where $V_0=\sigma^3/\sqrt{2}$ is the volume per particle at close packing. The relation between density and V/V_0 is therefore

$$n\sigma^3=\frac{\sqrt{2}}{V/V_0}\ .$$

The largest wavelength of the fluctuations that can be studied is, of course, the cell dimension itself. The wave number k is related to the wavelength λ by $k=2\pi/\lambda$. It is convenient to measure the wave number in terms of $k\sigma$, so that the smallest value of $k\sigma$ is

$$\min k\sigma=2\pi\left[\frac{\sqrt{2}}{NV/V_o}\right]^{1/3}\ .$$

Table I specifies the three density states investigated

TABLE I. Range of variables investigated.

V/V_0	$n\sigma^3$	$g(\sigma)$	l/σ	$k\sigma$	λ/l
10	0.144	1.21	1.31	0.41[a]	11.6
				5.36	0.9
3	0.471	2.06	0.23	0.62	44.
				0.31[b]	
				19.71	1.4
1.6	0.884	4.98	0.05	0.76	162.0
				0.38[b]	
				100.2	1.2

[a]The two entries for each density correspond to the minimum and maximum values investigated in the simulation study for 500 particles.

[b]Minimum value for 4000 particles.

and the range of $k\sigma$ that was studied. That range is comparable to the one that is covered by neutron diffraction experiments on liquid argon; namely, from about 0.3 to 20.

The highest-density state in Table I is close to the freezing density of the liquid, $V/V_0=1.50$. The intermediate density, $V/V_0=3$, is in the dense fluid region since, in the presence of a small attractive potential, the liquid-gas critical transition would occur at about $V/V_0=5$. By the same token the low-density state, $V/V_0=10$, is at about half the critical density; thus, it is still far from being a dilute gas.

Another characteristic length in the system besides that determined from V/V_0 or σ is the collision mean free path given by $l=[\sqrt{2}\pi n\sigma^2 g(\sigma)]^{-1}$, where $g(\sigma)$ is the pair distribution function at contact. Both l/σ and $g(\sigma)$ are also given in Table I. Whereas $k\sigma$ is a more natural dimensionless variable to express structural correlations, kl is a more appropriate variable for characterizing dynamic correlations. A small kl means that collisions are frequent, a necessary condition for the validity of hydrodynamics, while a large kl means that collisions are rare and unimportant compared to free-flow effects. Furthermore, the collision parameter $y=1/\sqrt{2}kl$ is often used in kinetic-theory calculations[11] to indicate whether the hydrodynamic regime ($y\geq 3$), the kinetic regime ($y\sim 1$), or the free-particle regime ($y\leq 3$) is the appropriate model.

In the simulation procedure the desired time correlation function, for example, the intermediate-scattering function $F(k,t)$, defined as

$$F(k,t)=\frac{1}{N}\left\langle \sum_{p,q}\exp\{i\vec{k}\cdot[\vec{R}_p-\vec{R}_q(t)]\}\right\rangle ,$$

where $R_j(t)$ is the position of particle j at time t and the angular brackets denote ergodic average, was generated at prescribed k values and at about 100 fixed time intervals. The results were then averaged over a number of time origins, separated by about one mean-collision time. The Enskog mean-collision time

$$\tau_E=[4\sqrt{\pi}n\sigma^2 v_0 g(\sigma)]^{-1}$$

is introduced for the purposes of measuring time in a dimensionless variable $s=t/\tau_E$, where v_0 is a velocity defined through $v_0^2=k_BT/m$. The length of a run was typically 4×10^4 collisions per particle for both the 500- and 4000-particle system. The N dependence of the results is given by the comparison shown in Fig. 1. The differences are almost within the combined statistical uncertainties.

Statistical fluctuations in the time correlation functions have been estimated at various times along the decay of each function. By assuming that the successive average values of the function over 10^6 collisions can be treated as uncorrelated, an absolute accuracy of the initially normalized correlation function of typically 0.02 or less was established. This uncertainty is indicated by the error bars in all figures.

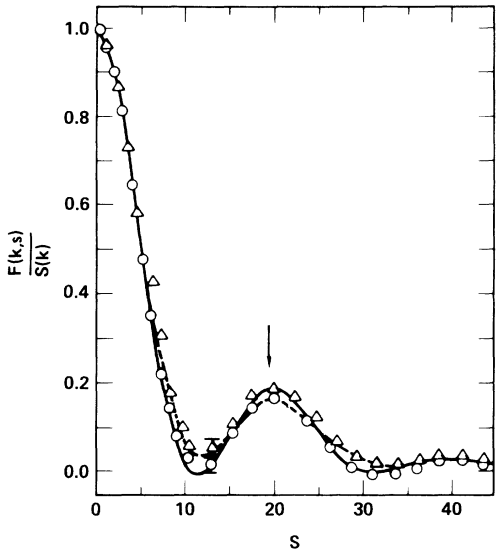

FIG. 1. Normalized intermediate-scattering function $F(k,s)$ of a hard-sphere fluid at $V/V_0=3$ and $k\sigma=0.62$ for 500 (circles) and 4000 (triangles) particles. Arrow indicates the time for a sound wave to travel the length of the 500-particle cell. Solid line represents the kinetic-theory result and the dashed line represents the hydrodynamic results. Error bars are indicated.

The frequency spectra are obtained by Fourier transforming the time functions and are expressed in terms of the dimensionless frequency variable $\tilde{\omega}=\omega\tau_E/k\sigma$. Because the time correlations were not smoothed before transforming, the frequency spectra show structure due to the noise present in the correlation functions as well as that due to truncation of the data.

As input for the hydrodynamic theory, the generalized thermodynamic properties and the wavelength-dependent transport coefficients are required. These have previously been determined for hard-sphere systems.[9] As input for the kinetic theory, the generalized thermodynamic properties derived from the static structure factor $S(k)$ [the Fourier spatial transform of the pair distribution function $g(r)$] are needed. The transport coefficients are determined by the kinetic theory itself and, hence, consistent with that theory, assume the

Enskog values. $S(k)$ can be obtained from the initial value of the intermediate-scattering function. The values generated in the present study are compared with the Percus-Yevick approximation[12] in Fig. 2. The agreement is generally within a few percent except at the highest density ($V/V_0=1.6$) and small $k\sigma$, where $S(k)$ is itself small. As is well known, Percus-Yevick is in error by about 20% in that region. Figure 2 also provides a useful guide to structural effects on fluctuations. The region of wave number where structural effects are expected to be strongest is near the first peak, which is called the first diffraction maximum. In the long-wavelength limit $S(k)$ approaches the value determined by the compressibility, as demonstrated in Fig. 2.

III. DENSITY CORRELATION FUNCTION

The Fourier transform of the intermediate-scattering function

$$S(k,\omega)=\int_{-\infty}^{\infty} dt\, e^{i\omega t}F(k,t)$$

is the dynamic structure factor, the quantity directly measured in an inelastic neutron or light scattering experiment. Much of the present knowledge about the behavior of $S(k,\omega)$ and $F(k,t)$ has been derived from neutron scattering measurements[13,14] and molecular-dynamics simulations on fluids with continuous potentials.[15,16] This neutron data cannot be used to make an unambiguous test of dynamical theories that apply only for hard spheres and, hence, there is a need to generate molecular-dynamics data on $F(k,t)$ and $S(k,\omega)$ for hard spheres.

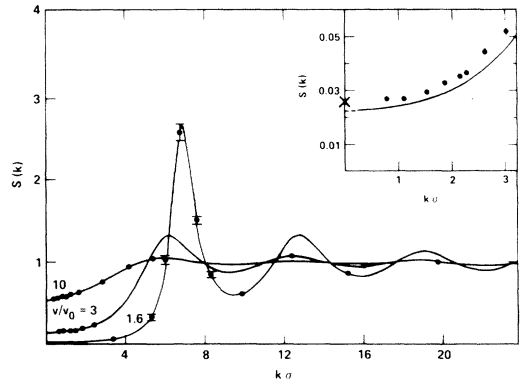

FIG. 2. Static structure factor $S(k)$ of a hard-spheres fluid at three densities indicated by the values of V/V_0. Molecular-dynamics results (circle) are compared to the Percus-Yevick approximation (solid curve). Comparison at the highest density ($V/V_0=1.6$) and small $k\sigma$ values is shown on an enlarged scale as an insert. Statistical uncertainties of the data points without error bars are smaller than the size of the circles. The cross represents the results of a molecular-dynamics calculation of the compressibility.

The behavior of $F(k,t)$ for hard spheres at three densities and covering a wide range of wavelengths is shown in Fig. 3. In each case at the smallest $k\sigma$ value, the intermediate-scattering function decays in an oscillatory manner, the oscillations being much more pronounced at the two lower densities. Since the oscillatory behavior signifies a propagating collective excitation, it is apparent that density fluctuations or sound waves are more strongly damped at liquid densities. As can be seen at intermediate densities for the same value of the wavelength, collective mode propagation can be better sustained than at either lower or higher densities. Hence, lack of experimental confirmation of a propagating mode in liquid argon suggests that such confirmation should be attempted at intermediate densities. The observed monotonic decay of $F(k,t)$ at all densities at a wavelength corresponding to $k\sigma=1.52$ (some 80 times the mean free path at liquid densities or four times the diameter of the hard-sphere particle) indicates that the propagating mode is effectively completely damped at that and all smaller wavelengths.

At liquid densities the decay of $F(k,t)$ is seen in Fig. 3(a) to slow down dramatically at wavelengths close to the first diffraction maximum. This effect, known as de Gennes narrowing in neutron scattering,[17] arises from the strong spatial correlations in this wavelength region and is an indication of the sensitive dependence of dissipative processes on the fluid structure. As the wavelength coincides with subsequent peaks in the static structure factor, corresponding to further neighbor distances, slowing down effects in $F(k,t)$ can also be expected but not as severe.

Kinetic theory, as can be observed in Fig. 3(a), accounts remarkably well for the slowing down effect. This can be traced to the dominance of the mean-field term in the generalized Enskog kinetic equation at the diffraction maximum. The collisional term, which the kinetic theory approximates, makes only a relatively minor contribution at the wavelength of the diffraction maximum; however, that term makes the dominant contribution on either side of the diffraction maximum, which accounts for the observed discrepancies there. Nevertheless, the kinetic theory outside the diffraction-maxima region correctly predicts the general trend of the increasing rate of correlation function decay with decreasing wavelengths.

The comparison of the kinetic theory with the

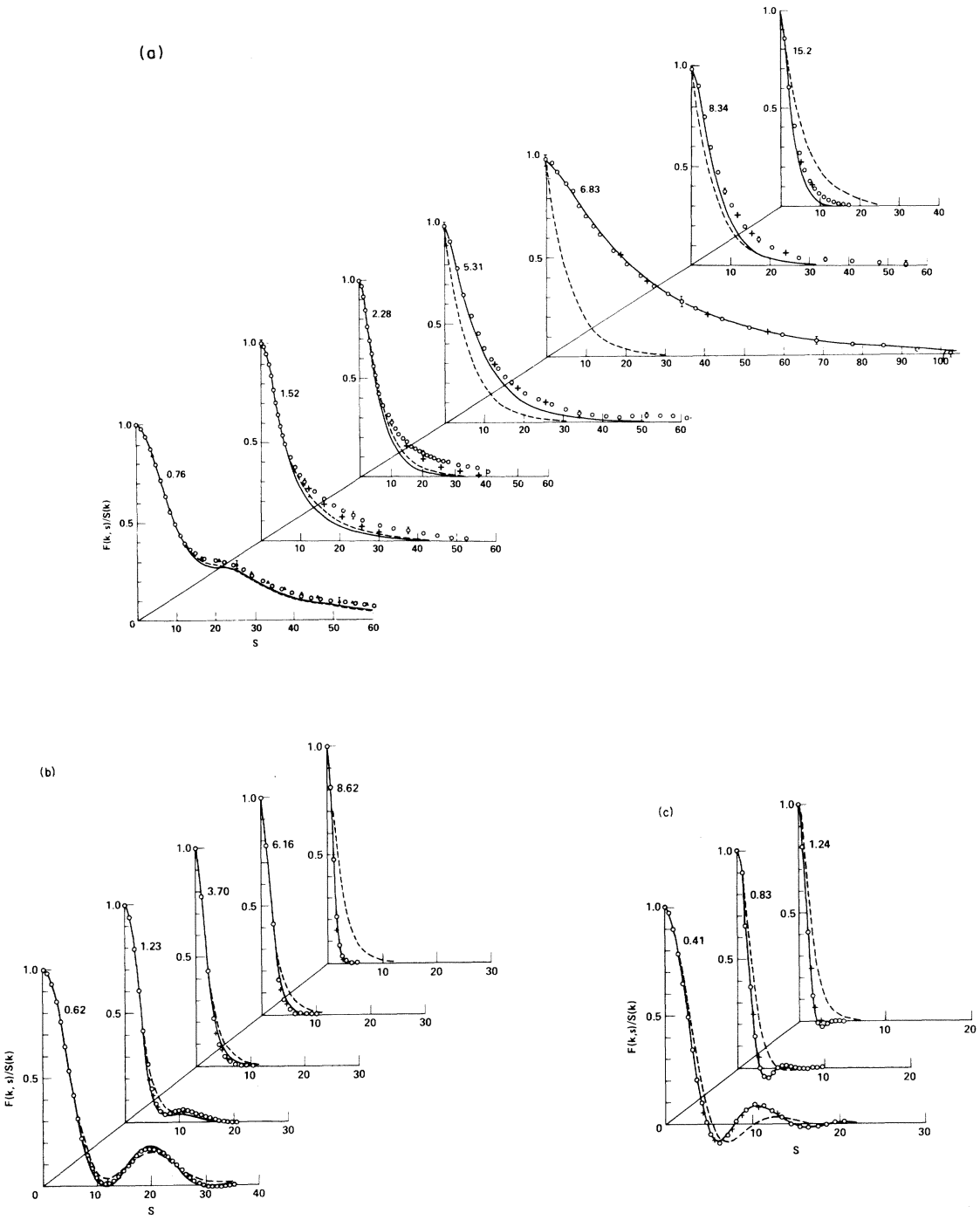

FIG. 3. Normalized intermediate-scattering function $F(k,s)$ of a hard-spheres fluid at (a) $V/V_0=1.6$, (b) $V/V_0=3.0$, (c) $V/V_0=10.0$ at various reduced wave numbers, $k\sigma$, obtained by molecular dynamics (circles) compared to kinetic theory (solid curves), hydrodynamics (dashed curves), and wavelength-dependent hydrodynamics (crosses). The value of $k\sigma$ is located to the right of each curve. Dimensionless time s is measured relative to the Enskog mean-collision time.

molecular-dynamic calculations is consistent with previous results. Previously it was found that the Enskog model gave quite accurate results in the long-wavelength limit at all but liquid densities, that is, for the transport coefficients themselves.[9] Since its extension to finite wavelengths should lead to at least as accurate results, it was found in the preceding paper that the generalized transport coefficients were also accurately evaluated at all but liquid densities and, hence, so should the neutron scattering function, as is confirmed in Figs. 3(b) and 3(c). At liquid densities the wavelength-dependent kinetic transport coefficients,[5] most importantly the viscosity, are too small in magnitude due to the neglect of the slow collective readjustment of the configurational liquid order in response to a stress fluctuation as the solid phase density is approached. This slow decay of the stress autocorrelation function at liquid densities has been colloquially dubbed the molasses effect. Its neglect, hence, leads to a too fast decay of $F(k,t)$ by the kinetic theory, as noted in Fig. 3(a).

At sufficiently short wavelength, however, this collective phenomena is eliminated since only a few particles are involved in the fluctuations and thus the kinetic theory becomes exact again. This is shown in detail in Fig. 4, which not only illustrates that for wavelengths of a few mean free paths kinetic theory is accurate, but that for wavelengths less than one mean free path the free-streaming approximation becomes quantitative. In that limit, collisions can be entirely neglected and $F(k,t)$ approaches a Gaussian function, $\exp[-(kv_0t)^2/2]$. That limit, $k\sigma > 100$ for $V/V_0 = 1.6$, is unfortunately beyond the reach of normal thermal neutron scattering experiments. However, the region where $F(k,t)$ decays slower than a Gaussian and thus $S(k,\omega)$ is, through the collision mechanism, narrower than the free-particle result has been observed in neutron scattering studies on pressurized hydrogen for the self-correlation function.[18,19]

At the other extreme of long wavelengths, agreement with hydrodynamics (including the observation of propagating modes) can be expected and is demonstrated in Fig. 5. Kinetic theory also reduces, at sufficiently long wavelength, to the hydrodynamic result, however, with the kinetic values of the transport coefficients. Since these are accurate except at the highest density, this accounts for the comparisons made in Fig. 5. At $V/V_0 = 1.6$ kinetic theory predicts a slightly more pronounced collective mode, characterized by a weak shoulder, primarily because the shear viscosity is too low by 40%, leading to less damping. On the other hand, the disagreement observed for the hydrodynamic theory with constant transport coefficients at low

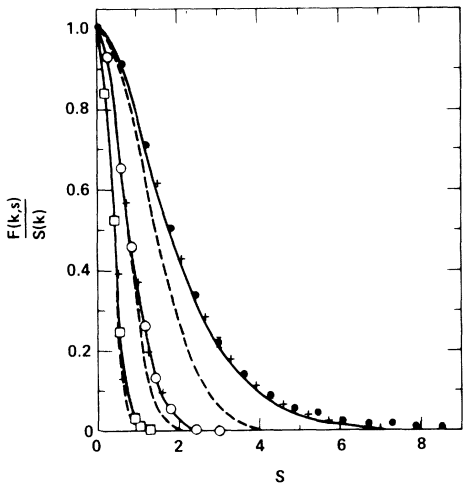

FIG. 4. Normalized intermediate-scattering function $F(k,s)$ of a hard-spheres fluid at $V/V_0 = 1.6$ and high reduced wave number $k\sigma = 25$ (closed circles), 50 (open circles), and 100 (squares), compared to kinetic theory (solid curve) and wavelength-dependent hydrodynamics (crosses). Dashed curves correspond to the free-streaming solutions.

density is due to the neglect of the wavelength dependence of the fluid properties when the mean free path is larger than the diameter of a particle. At higher densities at the same wavelength the mean free path is considerably smaller than the particle diameter and, as shown in the preceding paper, the fluid properties deviate, then, little from their long-wavelength limit. Correcting for the wavelength dependence leads to good agreement with molecular dynamics even at the lowest density.

Ordinary hydrodynamics at the highest density disagrees with molecular dynamics beyond the very-long-wavelength region in that the damping at short times is overestimated by the shear viscosity. This indicates that the relaxation of the density and shear fluctuations are comparable, so that it makes sense to introduce a time-dependent viscosity which interpolates between the Enskog value relevant at short times and the full value at long times. This is demonstrated in Fig. 6, where the intermediate-scattering function at high density is plotted on an expanded scale and is compared with two hydrodynamic calculations employing the two different viscosities. The figure shows that hydrodynamics using Enskog coefficients corresponds best with molecular dynamics at short times, while the hydrodynamic calculation which uses the correct high-

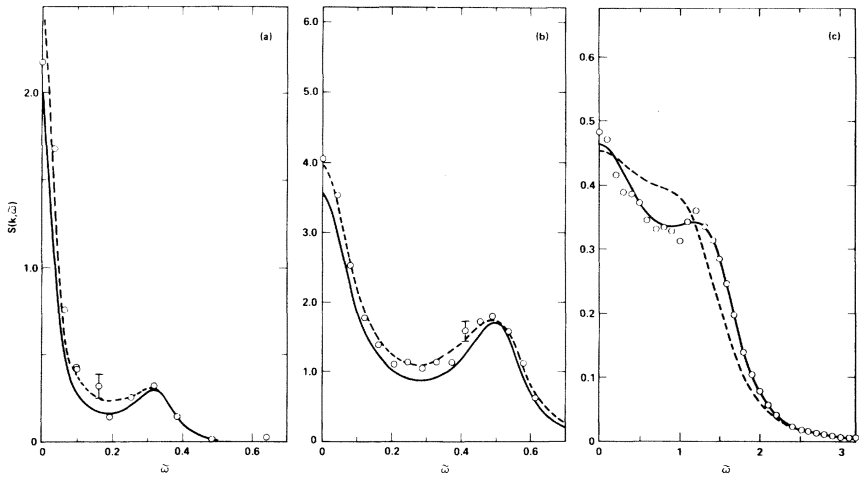

FIG. 5. Dynamic structure factor $S(k,\omega)$ of hard-spheres fluids at low wave number and three different densities, (a) $V/V_0=1.6$, $k\sigma=0.38$, (b) $V/V_0=3$, $k\sigma=0.44$, (c) $V/V_0=10$, $k\sigma=0.41$, by molecular dynamics (circles) compared to kinetic theory (solid curve) and hydrodynamics (dashed curve).

density values for the transport coefficients corresponds best with molecular dynamics at long times. At intermediate times, an interpolation is required. In this density and wavelength regime, one, hence, needs a nonlocal in time theory, but spatial nonlocality is not required. Such time-dependent transport coefficients are readily available from the time evolution of the autocorrelation functions.

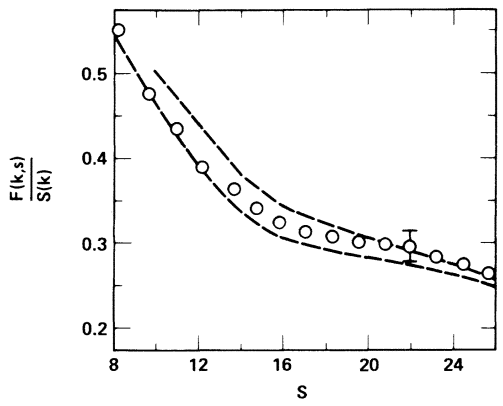

FIG. 6. Intermediate-scattering function for hard spheres at a density corresponding to $V/V_0=1.6$ and a wave number $k\sigma=0.76$ as a function of mean collisions s. Molecular-dynamics data are given by the circles, the upper dashed curve represents hydrodynamics using the correct values of the transport coefficients, and the lower dashed curve represents hydrodynamics using Enskog values for the transport coefficients.

On the other hand, spatially nonlocal hydrodynamics, where the fluid properties are only wavelength dependent, is applicable whenever the hydrodynamic relaxation times $1/k^2\nu$ are longer than the dissipative relaxation times of the transport processes, particularly the kinematic viscosity ν (see Figs. 3 and 4). For hard spheres this leads to the accurate prediction of $S(k,\omega)$ at all wavelengths greater than the mean free path by wavelength-dependent hydrodynamics except at the highest fluid densities. At high densities the viscous relaxation time is quite long and the hydrodynamic relaxation time is not long enough unless $k\sigma$ is greater than 5 or less than 0.3. As Figs. 3(a) and 4 show, from $k\sigma$ of 5 to the highest investigated value of 100, agreement with molecular dynamics is obtained. In that region of wavelengths the viscosity reaches its limiting value in the order of a collision and hydrodynamic relaxation times are long in comparison. At long wavelength, below $k\sigma$ values of 0.3, $1/k^2\nu$ becomes sufficiently large so that it exceeds the slow viscous relaxation time (of the order of 100 collisions); in that case ordinary hydrodynamics with wavelength-independent fluid properties works. As pointed out in the previous paragraph, in the region of $k\sigma$ between 0.3 and about 1.0, at high density, the two relevant relaxation times are comparable so that the time or frequency dependence of the fluid properties must be introduced to obtain a quantitative theory; however, the wavelength dependence can be ignored. In the region of $k\sigma$ between 1 and 5 both nonlocality in space and time are required to express the decay of fluctuations. If such wavelength- and

frequency-dependent fluid properties were introduced into fluctuating hydrodynamics, then $F(k,t)$ would be exactly reproduced, since such fluid properties were determined from $F(k,t)$ itself. It is in this region between $k\sigma$ of 0.3 and 5 and time scales between 10 and 50 collisions per particle that viscoelastic phenomena are observed. Because of the overwhelming importance of the wavelength dependence of the viscosity, introducing the wavelength dependence of fluid properties only through the thermodynamic properties derivable from $S(k)$ leads to only insignificant improvements over the predictions of ordinary hydrodynamics.[10]

IV. LONGITUDINAL CURRENT CORRELATION FUNCTION

An alternative method by which to represent the density fluctuations is in terms of the longitudinal current correlation function $J_l(k,t)$ defined as

$$J_l(k,t)=\frac{1}{N}\left\langle \sum_{p,q} v_p^z v_q^z(t)\exp\{i\vec{k}\cdot[\vec{R}_p-\vec{R}_q(t)]\}\right\rangle ,$$

where v_i^z is the velocity component of particle i parallel to k. By virtue of the equation of continuity, J_l can be simply expressed in terms of the density correlation function

$$J_l(k,t)=-\frac{1}{k^2}\frac{d^2}{dt^2}F(k,t)$$

or equivalently in frequency space as

$$J_l(k,\omega)=\frac{\omega^2}{k^2}S(k,\omega) .$$

The ω^2 factor weights the high-frequency regime of $S(k,\omega)$ more heavily while suppressing the importance of the low-frequency behavior. For this reason J_l is convenient for the discussion of propagating modes.

The time correlation function $J_l(k,t)$ has a heavily damped oscillatory behavior as seen in Fig. 7. It can again be observed that ordinary hydrodynamics overestimates damping and kinetic theory underestimates damping. It is convenient to discuss the characteristics of propagating modes in terms of the frequency and width of the peak in $J_l(k,\omega)$. Such results in terms of the reduced frequency are shown in Fig. 8. The scatter in the molecular-dynamics data can be attributed to the error incurred by Fourier transforming the raw data for $J_l(k,t)$ as well as some uncertainty in locating the peak position of a broad spectrum. At small k, the peak frequency varies with k as ck, where c is the adiabatic sound speed. As k increases, deviation from the long-wavelength behavior (called dispersion) sets in and,

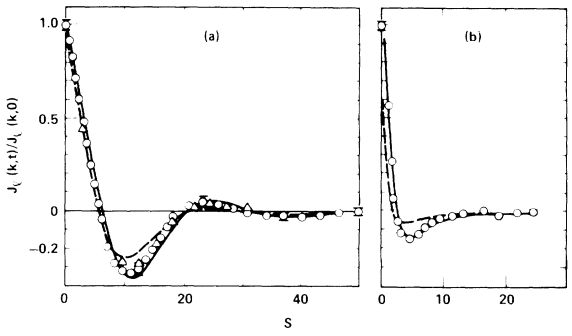

FIG. 7. Normalized longitudinal current correlation function $J_l(k,s)$ of a hard-spheres fluid at $V/V_0=1.6$ and at two wave numbers (a) $k\sigma=0.76$ and (b) 2.28 by molecular dynamics (circles) compared to kinetic theory (solid curve) and hydrodynamics (dashed curve).

as can be seen from Fig. 8, this occurs at wavelengths corresponding to $k\sigma\geq 1$, that is, only at wavelengths shorter than a few hard-sphere diameters, consistent with earlier observations.

Furthermore, Fig. 8 shows that the dispersion in the effective propagation speed is negative. Peak frequencies observed in rare-gas fluids, on the other hand, show a positive dispersion at wavelengths larger than the peak in the structure factor, while beyond that a sharply negative dispersion is found.

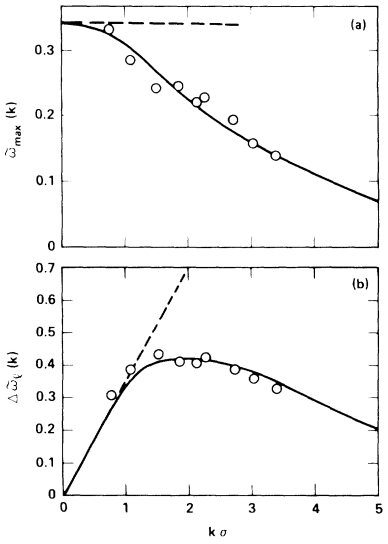

FIG. 8. Peak position (a) and the full width at half maximum (b) of the longitudinal current correlation function $J_l(k,s)$ of a hard-spheres fluid at $V/V_0=1.6$ by molecular dynamics (circles), kinetic theory (solid curve), and hydrodynamics (dashed curve).

For hard spheres no such positive dispersion has been found at the highest density and longest wavelength investigated, as is shown in more detail in Fig. 9. The importance of finding such positive dispersion is that it would yield evidence for the existence of the long-time tail in the autocorrelation function of the transport coefficients in the neutron scattering function. Since such tails could not be observed at the highest density in the autocorrelation functions for the transport coefficients themselves, for the largest system that could be reasonably investigated by molecular dynamics, it is not surprising that they cannot be detected in $S(k,\omega)$ either; such evidence presumably can be found by investigating still larger systems at longer wavelength.

At the lower density of $V/V_0=3$, the situation is more favorable for molecular dynamics since the velocity autocorrelation function, though not the more crucial stress autocorrelation function, gives clear evidence of a long-time tail. Indeed, as Fig. 9 shows, the data are consistent at that density with a weak positive dispersion predicted by a theory that takes the long-time tail into account.[20,23] The relatively large uncertainty in the data, in spite of the rather lengthy calculation, derives partially from the error in the graphical location of the sound speed as the peak in the Fourier transform of the longitudinal correlation function. However, determination of the sound speed by analyzing the molecular-dynamics data by generalized hydrodynamics led to identical results. It should be emphasized that the data are also consistent with a zero slope (wavelength-independent sound speed) prediction and, hence, it appears that only very precise data will be able to give evidence for long-time tails in the sound speed.

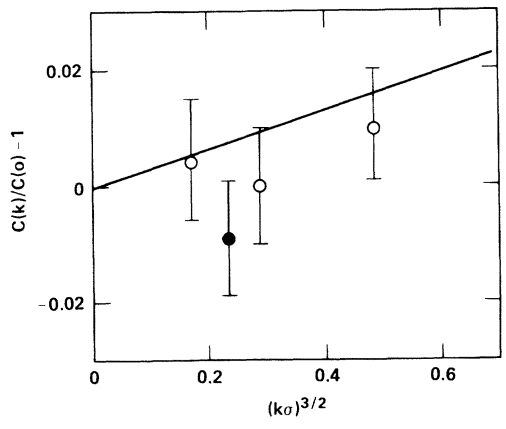

FIG. 9. Adiabatic sound speed as a function of wave number for two hard-spheres systems: $V/V_0=1.6$ (solid circle) and $V/V_0=3.0$ (open circles). Solid line is the result of a theoretical calculation for $V/V_0=3.0$

The width of the propagating mode, also given in Fig. 8, is reasonably well accounted for by kinetic theory even at liquid densities. The incorrect values of the transport coefficients lead to too small a slope in the low-wavelength behavior of the width. At larger $k\sigma$ the width behaves like the damping of zero sound. From the calculation of the width at the two lower densities, it can be concluded that the general dependence on $k\sigma$ is quite similar except that deviations from the long-wavelength behavior starts at somewhat lower $k\sigma$ values as the fluid density is lowered.

V. TRANSVERSE-CURRENT CORRELATION FUNCTION

Fluctuations in the transverse-current density are described by

$$J_t(k,t)=\frac{1}{N}\left\langle \sum_{p,q} v_p^x v_q^x(t)\exp\{i\vec{k}\cdot[\vec{R}_p-\vec{R}_q(t)]\}\right\rangle ,$$

where v_i^x is the component of the velocity of the ith particle perpendicular to k. Its Fourier transform will be denoted by $J_t(k,\omega)$. Although this quantity cannot be measured in a fluid by neutron scattering, it is of considerable interest because of its fundamental relation to the shear viscosity. In the long-wavelength limit $J_t(k,t)$ satisfies the diffusion equation with the kinematic viscosity ($\nu=\eta/\rho$, where ρ is the mass density) as the dissipative coefficient. Previous molecular-dynamics simulations with a Lennard-Jones potential near the triple point have revealed a resonant structure in $J_t(k,\omega)$ at $k\sigma$ above ~ 1.7 which has been interpreted as evidence of shear-wave propagation.[14] There exists no simulation at lower densities, so it is not known whether such excitations also appear in dense gases.

In Fig. 10 hard-sphere data on $J_t(k,t)$ at high density are shown at two wave numbers. The correlation functions decay monotonically at the lowest value of $k\sigma=0.76$, but at $k\sigma=2.28$, $J_t(k,t)$ shows a negative region near 12 mean-collision times. This is also about the time when persistent correlations manifest themselves in $F(k,t)$ (see Fig. 3). The oscillatory behavior in $J_t(k,t)$ already sets in at $k\sigma=1.52$ (not shown) and hence agrees well with the critical wave number for shear-wave propagation found in the earlier molecular-dynamics simulation. The time at which $J_t(k,t)$ becomes negative decreases rapidly with increasing wave number, but then remains constant near the first diffraction maximum. The negative feature of $J_t(k,t)$ is not very pronounced and appears to be qualitatively wave-number independent. At wave numbers beyond the

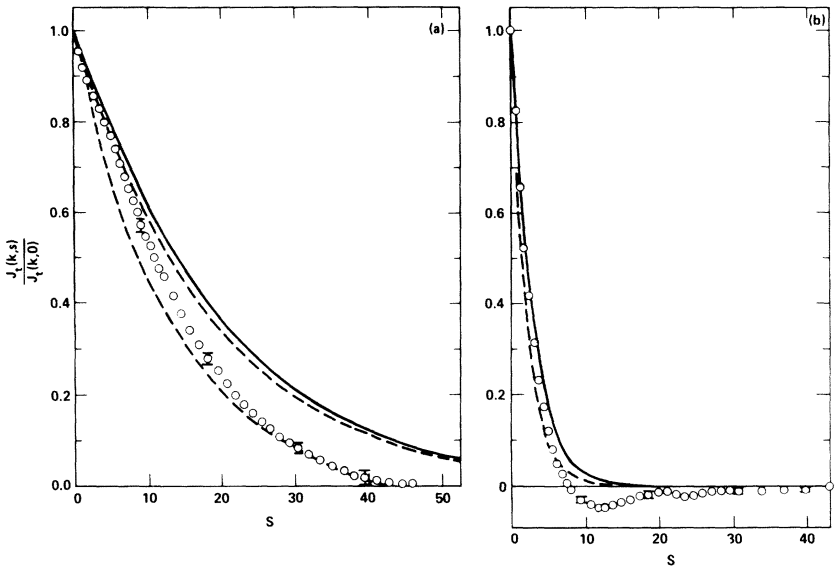

FIG. 10. Normalized transverse-current correlation function $J_t(k,s)$ of a hard-spheres fluid at $V/V_0=1.6$ at two different wavelengths (a) $k\sigma=0.76$ and (b) 2.28 by molecular dynamics (circles) compared to kinetic theory (solid curves) and hydrodynamics (dashed curves). At $k\sigma=0.76$ the upper dashed curve corresponds to a relaxation governed by the Enskog viscosity, while the lower dashed curve uses the correct viscosity.

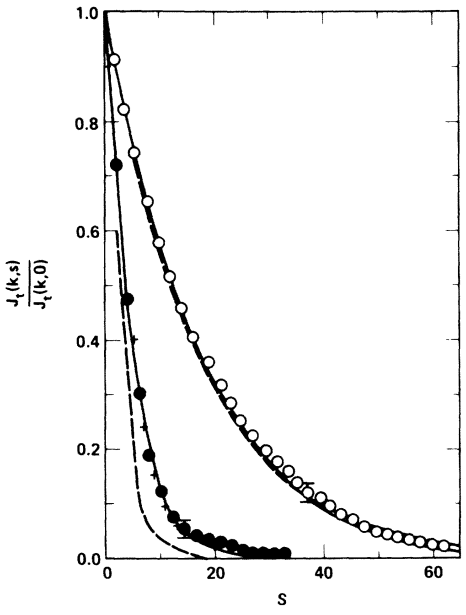

FIG. 11. Normalized transverse-current correlation function $J_t(k,s)$ of a hard-spheres fluid at $V/V_0=3.0$ at two different wavelengths, $k\sigma=0.62$ (open circles) and 1.23 (closed circles) by molecular dynamics compared to kinetic theory (solid curves), hydrodynamics (dashed curves), and wavelength-dependent hydrodynamics (crosses).

diffraction peak, the decay of the transverse-current correlation functions becomes nonoscillatory, indicating that the fluid will not support shear waves at these wavelengths.

Neither kinetic theory nor conventional hydrodynamics can account for the shear-wave propagation phenomenon. As Fig. 10 shows, even at the lowest $k\sigma$ value, where the oscillatory behavior has not yet set in, there is, nevertheless, a significant

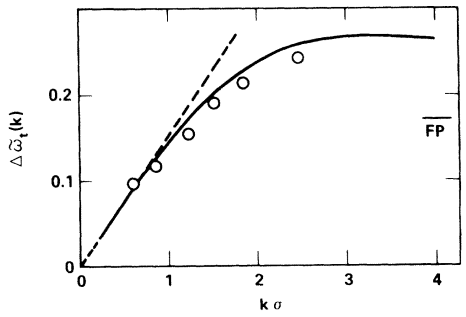

FIG. 12. Full width at half maximum of the peak in the frequency spectrum of the transverse-current correlation function $J_t(k,\omega)$ of a hard-spheres fluid at $V/V_0=3$. Molecular-dynamics results (circles) are compared to the kinetic theory (solid curve) and hydrodynamics (dashed curve). The short-wavelength limiting value is indicated by FP (free particle).

TABLE II. Intermediate-scattering function and the transverse-current autocorrelation function at $V/V_0=1.6$.[a]

	$k\sigma=0.380$ $\Delta s=4.178$		$k\sigma=0.760$ $\Delta s=1.671$		$k\sigma=2.28$ $\Delta s=1.233$	
$\frac{s}{\Delta s}$	$\frac{F(k,s)}{F(k,0)}$	$\frac{J_t(k,s)}{J_t(k,0)}$	$\frac{F(k,s)}{F(k,0)}$	$\frac{J_t(k,s)}{J_t(k,0)}$	$\frac{F(k,s)}{F(k,0)}$	$\frac{J_t(k,s)}{J_t(k,0)}$
0	1.00	1.00	1.00	1.00	1.00	1.00
1	0.95	0.95	0.97	0.92	0.92	0.67
2	0.83	0.88	0.89	0.84	0.77	0.41
3	0.67	0.82	0.78	0.75	0.63	0.23
4	0.51	0.76	0.67	0.67	0.51	0.12
5	0.40	0.70	0.56	0.60	0.43	0.05
6	0.33	0.64	0.47	0.53	0.36	0.01
7	0.32	0.59	0.41	0.47	0.32	−0.02
8	0.34	0.54	0.36	0.41	0.28	−0.04
9	0.38	0.50	0.33	0.35	0.25	−0.04
10	0.41	0.46	0.32	0.30	0.22	−0.05
11	0.42	0.42	0.31	0.26	0.20	−0.04
12	0.42	0.39	0.31	0.22	0.18	−0.04
13	0.39	0.36	0.31	0.19	0.16	−0.03
14	0.34	0.34	0.30	0.16	0.15	−0.03
15	0.30	0.31	0.29	0.14	0.13	−0.02
16	0.26	0.29	0.27	0.12	0.12	−0.02
17	0.23	0.27	0.26	0.10	0.11	−0.02
18	0.21	0.25	0.24	0.08	0.11	−0.01
19	0.21	0.23	0.22		0.10	
20	0.21	0.22	0.21		0.09	
21	0.22	0.20	0.19			
22	0.22	0.18	0.17			
23	0.22	0.17	0.16			
24	0.21	0.16	0.15			
25	0.20	0.14	0.13			
26	0.18	0.13	0.12			
27	0.16	0.12	0.12			
28	0.14	0.11	0.11			
29	0.13	0.10	0.10			

[a]The statistical uncertainty is 0.01

discrepancy between kinetic theory and molecular dynamics. Figure 10(a) further demonstrates the need to introduce a time-dependent relaxation rate into hydrodynamics by comparing the rate of relaxation of two hydrodynamics calculations as was done in Fig. 6. The difficulty with kinetic theory and ordinary hydrodynamics is most dramatically demonstrated by the absence of memory effects which can cause the correlation function to become negative. A similar effect has previously been noted for the velocity autocorrelation function at high fluid densities, which, for a qualitative explanation, requires the introduction into hydrodynamics of viscoelastic behavior, that is, time-dependent transport coefficients.

In the dense gas, at $V/V_0=3$, molecular-dynamics data show no evidence of shear-wave excitations. Under these circumstances kinetic theory as well as wavelength-dependent hydrodynamics is quantitatively accurate in describing $J_t(k,t)$, as seen in Fig. 11. For the dense gas, the full width at half maximum of $J_t(k,t)$ is shown in reduced frequency units in Fig. 12. From hydrodynamics one expects that, at long wavelengths,

$$J_t(k,\omega)\sim\frac{1}{\pi}\frac{\eta k^2/\rho}{\omega^2+(\eta k^2/\rho)^2}$$

so that its full width at half maximum is just $2\eta k^2/\rho$. At the lowest values of $k\sigma$ the molecular-

TABLE III. Intermediate-scattering function and the transverse-current auto correlation function at $V/V_0 = 3.0$.[a]

$\frac{s}{\Delta s}$	$k\sigma=0.308$ $\Delta s=2.354$ $\frac{F(k,s)}{F(k,0)}$	$k\sigma=0.308$ $\Delta s=5.885$ $\frac{J_t(k,s)}{J_t(k,0)}$	$k\sigma=0.616$ $\Delta s=1.177$ $\frac{F(k,s)}{F(k,0)}$	$k\sigma=0.616$ $\Delta s=2.354$ $\frac{J_t(k,s)}{J_t(k,0)}$
0	1.00	1.00	1.00	1.00
1	0.96	0.93	0.97	0.91
2	0.86	0.86	0.87	0.80
3	0.71	0.79	0.74	0.70
4	0.54	0.72	0.58	0.61
5	0.36	0.67	0.42	0.53
6	0.20	0.61	0.28	0.47
7	0.08	0.56	0.17	0.41
8	0.01	0.52	0.09	0.36
9	−0.02	0.48	0.05	0.31
10	0.00	0.44	0.04	0.28
11	0.06	0.40	0.05	0.24
12	0.14	0.37	0.08	0.21
13	0.22	0.34	0.11	0.19
14	0.30	0.31	0.14	0.16
15	0.39	0.29	0.17	0.14
16	0.36	0.26	0.19	0.13
17	0.30	0.24	0.19	0.11
18	0.23	0.22	0.18	0.09
19	0.16	0.20	0.17	0.08
20	0.10	0.18	0.14	0.07
21	0.05	0.17	0.12	
22	0.02	0.16	0.09	
23	0.01	0.14	0.07	
24	0.01	0.13		
25	0.02	0.12		
26		0.11		
27		0.10		
28		0.09		
29		0.09		

[a]The statistical uncertainty is 0.01.

dynamics results are in agreement with this behavior. Deviation from hydrodynamics behavior, as expected, sets in at about $k\sigma \sim 1$, the width then changes continuously from a k^2 dependence to an essentially linear dependence at $k\sigma \sim 3$. At still larger $k\sigma$ it decreases gradually and eventually approaches the free-particle limit.

ACKNOWLEDGMENTS

We thank Mary Ann Mansigh for expert handling of the computer codes. This work was performed in part under the auspices of the U.S. Department of Energy by the Lawrence Livermore National Laboratory under contract No. W-7405-ENG-48 and the National Science Foundation. One of us (S.Y.) is grateful to the Alexander von Humboldt Foundation for an award and the Institute für Festkörperforschung, Kernforschungsanlage Jülich, for hospitality during manuscript preparation.

APPENDIX

This appendix contains the raw molecular-dynamics data for the intermediate-scattering function $F(k,t)$ and the transverse-current autocorrelation function $J_t(k,t)$ for 4000 particles at selected values of $k\sigma$ and two densities. Table II gives these functions, which are normalized by their initial values, at three $k\sigma$ values for $V/V_0 = 1.6$ as a function of $s/\Delta s$, where s is time measured in mean collisions and Δs is the interval in mean collisions between each entry. The statistical error is ± 0.01 for all entries. Table III is the same as Table II except at $V/V_0 = 3.0$.

[1]For a review, see J. R. D. Copley and S. W. Lovesey, Rep. Prog. Phys. 38, 461 (1975); P. Schofield, in *Statistical Mechanics,* edited by K. Singer (Chemical Society, London, 1975), Vol. II.

[2]For monographs, see J. P. Hansen and I. R. McDonald, *Theory of Simple Liquids* (Academic, London, 1976); N. H. March and M. P. Tosi, *Atomic Dynamics in Liquids* (Halsted-Wiley, New York, 1977); J.-P. Boon and S. Yip, *Molecular Hydrodynamics* (McGraw-Hill, New York, 1980).

[3]R. Mountain, Rev. Mod. Phys. 38, 205 (1966); L. Kadanoff and P. C. Martin, Ann. Phys. (N.Y.) 24, 419 (1963); P. C. Martin, *Measurements and Time Correlation Functions* (Gordon and Breach, New York, 1968).

[4]For early work, see C.-H. Chung and S. Yip, Phys. Rev. 182, 323 (1969); A. Z. Akcasu and E. Daniels, Phys. Rev. A 2, 962 (1970); N. K. Ailawadi, A. Rahman, and R. Zwanzig, *ibid.* 4, 1616 (1971); a more recent summary is in Chap. 6 of Boon and Yip, Ref. 2. For calculations using a kinetic equation, see I. M. de Schepper and E. G. D. Cohen, *ibid.* 22, 287 (1980).

[5]J. R. Dorfman and H. van Beijeren, in *Statistical Mechanics, Part B: Time Dependent Processes,* edited by B. J. Berne (Plenum, New York, 1977); G. W. Ford

and J. Foch, in *Studies in Statistical Mechanics,* edited by G. E. Uhlenbeck and J. de Boer (North-Holland, Amsterdam, 1970), Vol. 5, p. 103; E. P. Gross, in *Lectures in Theoretical Physics-Kinetic Theory,* edited by W. Brittin, A. O. Barut, and M. Guenin (Gordon and Breach, New York, 1967), Vol. 9C, p. 171. For a recent discussion, see I. M. de Schepper and E. G. D. Cohen, J. Stat. Phys. 27, 223 (1982).

[6]G. F. Mazenko, Phys. Rev. A 9, 360 (1974); J. R. Dorfman, in *Fundamental Problems in Statistical Mechanics,* edited by E. G. D. Cohen (North-Holland, Amsterdam, 1975), Vol. 3, p. 277; Y. Pomeau and P. Resibois, Phys. Rep. 2, 63 (1975); L. Sjogren and A. Sjolander, Ann. Phys. (N.Y.) 110, 122 (1978); S. Yip, Ann. Rev. Phys. Chem. 30, 547 (1979); E. Leutheusser, J. Phys. C 15, 2801 (1982); 15, 2827 (1982).

[7]For derivations, see L. Blum and J. L. Lebowitz, Phys. Rev. 185, 273 (1969); J. L. Lebowitz, J. K. Percus, and J. Sykes, *ibid.* 188, 487 (1969); G. F. Mazenko, T. Y. C. Wei, and S. Yip, Phys. Rev. A 6, 1981 (1972); H. H. U. Konijnendijk and J. M. J. van Leeuwen, Physica (Utrecht) 64, 342 (1973).

[8]S. Yip, W. E. Alley, and B. J. Alder, J. Stat. Phys. 27, 201 (1982); for other approaches, see I. M. de Schepper and E. G. D. Cohen, Refs. 4 and 5, and J. W. Dufty, M. J. Lindenfeld, and G. E. Garland, Phys. Rev. A 24, 3212 (1981).

[9]B. J. Alder, D. M. Gass, and T. E. Wainwright, J. Chem. Phys. 53, 3813 (1970); W. E. Alley, B. J. Alder, Phys. Rev. A 27, 3158 (1983).

[10]J. Keizer and M. Medina-Noyola, Physica (Utrecht) 115A, 301 (1982).

[11]M. Nelkin and A. Ghatak, Phys. Rev. 135, A4 (1964); S. Yip and M. Nelkin, *ibid.* 135, A1241 (1964); S. Yip, J. Acoust. Soc. Am. 49, 941 (1971).

[12]N. W. Ashcroft and J. Lekner, Phys. Rev. 145, 83 (1966).

[13]K. Skold, J. M. Rowe, G. Ostrowski, and P. D. Randolph, Phys. Rev. A 6, 1107 (1972); J. R. D. Copley and J. M. Rowe, *ibid.* 9, 1656 (1974).

[14]For reviews, see J. R. D. Copley and S. W. Lovesey, Ref. 1 and J.-P. Boon and S. Yip, Ref. 2.

[15]A. Rahman, Phys. Rev. 136, A405 (1964); Phys. Rev. Lett. 19, 420 (1967); in *Neutron Inelastic Scattering* (International Atomic Energy Agency, Vienna, 1968), Vol. 1, p. 561; D. Levesque and L. Verlet, Phys. Rev. A 2, 2514 (1970); D. Levesque, L. Verlet, and J. Kurkijarvi, Phys. Rev. A 7, 1690 (1973).

[16]For reviews, see I. R. McDonald, in *Microscopic Structure and Dynamics of Liquids,* edited by J. Dupuy and A. J. Dianoux (Plenum, New York, 1978); J.-P. Hansen, D. Levesque, and J. J. Weiss, in *Monte Carlo Methods in Statistical Physics,* edited by K. Binder (Springer, New York, 1979).

[17]P. G. de Gennes, Physica (Utrecht) 25, 825 (1959).

[18]M. Nelkin and A. Ghatak, Ref. 11.

[19]S.-H. Chen, Y. Lefevre, and S. Yip, Phys. Rev. A 8, 3163 (1972); D. Levesque, L. Verlet, and J. Kurkijarvi, Ref. 15.

[20]M. H. Ernst and J. R. Dorfman, J. Stat. Phys. 12, 311 (1975).

[21]I. M. de Schepper, P. Verkerk, A. A. van Well, and L. A. de Graaf, Short Wavelength Sound Modes in Liquid Argon, Interuniversitair Reactor Institut, Delft, The Netherlands (in press).

[22]J. Thomassen and M. H. Ernst (unpublished).

[23]I. M. de Schepper, J. Thomassen, and M. H. Ernst, Nonanalytic Dispersion Relations (in press).